Adsorption and bonding mechanism of a N,N′-di(*n*-butyl)quinacridone monolayer studied by density functional theory including semiempirical dispersion corrections

J.-H. Franke, V. Caciuc, L. F. Chi,* and H. Fuchs
Physikalisches Institut, Westfälische Wilhelms Universität Münster, Wilhelm-Klemm-Strasse 10, 48149 Münster, Germany
(Received 8 July 2008; published 31 October 2008)

The adsorption of a monolayer of N,N′-di(*n*-butyl)quinacridone on Ag(110) is studied by density functional theory including semiempirical dispersion corrections. The bonding mechanism is governed by the formation of an oxygen-Ag bond involving first-layer Ag atoms and the butyl chains are found to be folded away from the substrate in the most stable geometry. A small charge donation from the substrate to the lowest unoccupied molecular orbital is observed. Work-function changes are calculated for different adsorption energies, indicating a lowering of the work function by up to 0.85 eV. The semiempirical dispersion corrections give a large energy gain upon adsorption that is almost site unspecific. Accordingly the molecule-surface distance is reduced especially for weakly bound configurations. The induced change to the electronic structure in these cases also alters the calculated work function change significantly.

DOI: 10.1103/PhysRevB.78.165432 PACS number(s): 68.43.Fg, 71.15.Dx, 81.16.Dn

I. INTRODUCTION

In the last decade, the study of the self-assembled monolayers (SAMs) on surfaces has received considerable interest due to the possibility to employ this approach to develop molecule-based devices. For instance, electronic devices based on light-emitting diodes (OLEDs) are already present in the daily life as flat displays.[1] Another appealing possibility is to use organic molecules as functional building blocks in molecular electronic nanodevices.[2,3] In particular, this perspective opens the road to design electronic circuits at atomic scale and thus to avoid the size limit of the silicon-based microchip technology. In this context, promising experimental results have been obtained for single molecule diodes[4,5] or for organic field-effect transistors.[6–8]

From a theoretical point of view, a prerequisite in understanding the functionality of such molecular devices is to investigate the interaction mechanism of SAMs with the substrate in question. Such an analysis has been performed, for instance, for the self-assembled monolayers of π-conjugated molecules on Ag and Au(111) surfaces,[9,10] a monolayer of 3,4,9,10-perylene-tetracarboxylic-dianhydride (PTCDA) on the Ag(111) surface,[11] or a SAM of tetrahydroxyquinone molecules also on the Ag(111) substrate.[12]

The general physical picture emerged from these first-principles studies based on state-of-the art density functional theory (DFT) is that the adsorption mechanism of SAMs on metal surfaces depends on a subtle interplay between the strength of the intermolecular interactions and those between the adsorbate and the substrate. A special difficulty in describing correctly the magnitude of these interactions occurs when the molecules are physisorbed on the surface of interest.[13] In this case, the long-range van der Waals interactions play a crucial role in the SAM-substrate system and these dispersion effects are poorly described by the current exchange-correlation energy functionals such as local-density approximation (LDA) or generalized gradient approximation (GGA) used in DFT.[14,15] Of course, similar difficulties appear also when the molecule-molecule interactions in a monolayer are dominated by these dispersion (van der Waals) forces.

In practice, this delicate balance between molecule-molecule and molecule-substrate interactions can lead to a rich variety of adsorption geometries of SAMs on surfaces. For instance, a recent low-energy electron diffraction (LEED) and scanning tunneling microscopy (STM) study focused on the adsorption geometry of a N,N′-di(*n*-butyl)quinacridone (DBQA) monolayer on Ag(110) surface[16] revealed that, depending on the growth temperature, the DBQA monolayer can adopt a commensurate or incommensurate structure. In this study it was suggested that a commensurate structure is obtained when adsorbate-surface interactions dominate over the hydrogen-bonded intermolecular ones while the opposite is true for the incommensurate adsorption geometry.

However, the role of the van der Waals interaction on the adsorption process of DBQA on the Ag(110) substrate could not be assessed from the experimental data. Therefore, the basic aim of this study is to investigate the bonding mechanism of a DBQA monolayer on the Ag(110) surface by performing *ab initio* simulations on this system. To account for the missing dispersion effects in the standard implementations of the DFT, in our first-principles calculations we described the van der Waals forces using the semiempirical approach proposed by Grimme.[17] When included, the dispersion interactions lead to two major differences with respect to the results obtained only with DFT: (a) the adsorption (binding) energies are significantly increased and (b) the relaxation pattern of the DBQA monolayer is qualitatively different leading to important changes of the electronic structure of the adsorbate-surface system.

II. COMPUTATIONAL METHOD

A. General methodology

This study was performed using DFT as implemented in the program package VASP.[18–20] The exchange-correlation functional of Perdew, Burke, and Ernzerhof (PBE) was employed.[21] The PBE functional was chosen because it is known to model hydrogen bonding quite well[22] and param-

eters for a semiempirical dispersion correction are readily available. Because the underbinding of the GGA in general often causes problems for modeling weak adsorption processes on substrates, we tackled this problem by adding semiempirical dispersion corrections.[17] The valence-core interactions were modeled using the projector augmented wave method[23] as implemented in VASP.[24] The Kohn-Sham (KS) wave functions were expanded in a plane-wave basis set with a cutoff energy of 400 eV and the k mesh was sampled by the Γ point only. All structural relaxations were converged to forces of less than 10 meV/Å. For the DBQA monolayer adsorbed on Ag(110) the total energy was dipole corrected along the surface normal.

The Ag(110)-(4×6) surface is modeled by a periodic slab of five layers of Ag and 11 layers of vacuum to avoid spurious interactions between neighboring slabs. The geometry of the in-plane surface unit cell is that suggested by STM and LEED experiments performed on this system.[16] To obtain the ground-state adsorption geometry, the first two layers of the substrate were allowed to relax as well as all atoms in the molecules.

To evaluate the strength of the molecule-molecule and molecule-Ag(110) surface interactions, we calculated the corresponding binding energy. The binding energy of the DBQA monolayer (per molecule) in vacuum is calculated as

$$E_{\text{binding}}^{\text{mon}} = \frac{1}{2}(E_{\text{mon}} - 2E_{\text{DBQA}}) \tag{1}$$

and the adsorption energy per molecule of the monolayer adsorbed on the substrate is given by

$$E_{\text{binding}}^{\text{DBQA+Ag(110)}} = \frac{1}{2}(E_{\text{DBQA+Ag(110)}} - 2E_{\text{DBQA}} - E_{\text{Ag(110)}}), \tag{2}$$

with E_{DBQA}, E_{mon}, $E_{\text{Ag(110)}}$, and $E_{\text{DBQA+Ag(110)}}$ denoting the energies of the molecule, monolayer, substrate, and the whole monolayer-substrate system, respectively.

B. Implementation of semiempirical dispersion corrections

Although density functional theory is in principle able to give the correct ground-state energies of separated systems, it is well known that current commonly used generalized gradient approximations do not describe the dispersion part of the van der Waals forces correctly.[25] This inspired a lot of research toward alleviating this problem. Different strategies emerged, some of them trying to incorporate this electron correlation effect in a new exchange-correlation functional.

Andersson and co-workers[26–28] proposed a functional that was built from the formula of Rapcewicz *et al.*[29] Initially, it was restricted to isolated fragments such as atoms[26] or jellium substrates,[27] but later on a seamless version was developed.[15,14] Another scheme treats the long-range exchange exactly and short-range exchange by conventional GGA,[30] and additionally an all functional with a damping function for small length scales is included.[31–33] Numerous other approaches are available: Dobson and Dinte[34] exploited the charge conservation and reciprocity to derive a formula similar to Ref. 29. Lein *et al.*[35] proposed several approximations to the correlation functional derived from the adiabatic connection formula. Basanta *et al.*[36] suggested to treat van der Waals forces in an effective hopping approach in local-orbital DFT.

However many other groups proposed to treat the long-range interactions by supplementing conventional DFT functionals by a damped atom pairwise C_6R^{-6} correction (and possibly higher order terms) that recovers the correct asymptotic behavior at large distances.[37–45] The way in which the C_6 coefficients are obtained vary quite considerably within these approaches as does the theory used to model the short-range interaction and the damping functions. Elstner *et al.*[37] and Zhechkov *et al.*[38] employed density functional tight binding as the basis to which the long-range dispersion corrections are added. Wu and Yang[40] used different common density functionals and obtained atomic C_6 coefficients from molecular dipole oscillator strength distributions, also testing two different damping functions. Becke calculates the C_6 coefficients from the exchange hole.[42,43] For a more extensive review see, e.g., Refs. 41 and 46. A point worth mentioning for practical applications is the low computational cost of the empirical C_6R^{-6} approach. Especially in the case of very large systems such as the one under study here, this aspect is very important.

Grimme[47] developed a semiempirical dispersion correction scheme of the C_6R^{-6} form, with C_6 parameters taken initially from Wu and Yang.[40] Later, a new functional called B97-D was developed that was parameterized including a semiempirical correction of this form which was found to be very accurate for a large number of systems.[17,46] However the C_6 parameters found in this approach could also be used to supplement conventional GGAs with appropriate scaling factors s_6 (see below). We used this approach in conjunction with the PBE functional because we wanted to stick to the reliable PAWs generated using PBE that are available with the VASP code.

The energy in this scheme is divided into a DFT part and a dispersion part

$$E = E_{\text{DFT}} + E_{\text{disp}}. \tag{3}$$

The DFT energy is the result of a standard DFT calculation while the dispersion part is calculated as a pairwise sum over all atoms in a sphere of 20 Å diameter around each atom in the supercell, scaled by the global factor s_6:

$$E_{\text{disp}} = -s_6 \sum_T \sum_i \sum_j \frac{C_{6_{i,j}}}{R_{ij,T}^6} f_{dmp}(R_{ij,T}). \tag{4}$$

The summation over i and j runs over all atoms of the unit cell while the T summation runs over all translation vectors that are necessary to adhere to the periodic boundary conditions within a sphere of 20 Å. For T=0, the summation over j only runs from $i+1$ to the number of atoms in the supercell N_{at}. $R_{ij,T}$ is the distance between atom i in the main unit cell and atom j in a unit cell dislocated by the translation vector T. s_6 is 0.75 for the PBE functional. For further details on the C_6 coefficients and the damping function employed, the reader is referred to Ref. 17.

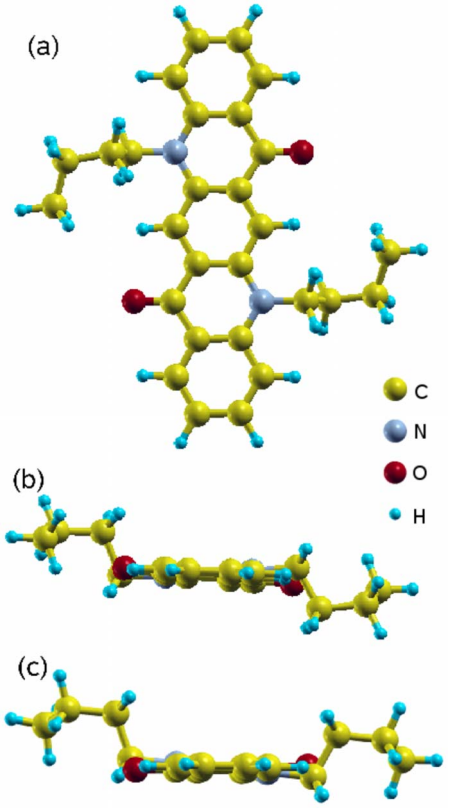

FIG. 1. (Color online) (a) and (b) Relaxed molecule from crystal structure ("arm down" configuration). (c) Configuration with both butyl chains pointing upwards (arm up configuration). All plots have been obtained using XCrysDen.

The simple form of the energy-correction term also leads to very simple forces that are then added to the Hellmann-Feynman forces obtained from the DFT-PBE calculation. The force for each atom i in the supercell is simply calculated as

$$\vec{F}_i = -\nabla E_{\text{disp}}, \tag{5}$$

also taking the correct counterforces for atoms inside the supercell into account. To investigate the role of the structural relaxations of molecules adsorbed on surfaces induced by dispersion corrections on the electronic structure of the molecule-substrate interface, this semiempirical approach as formulated by Grimme[17] was implemented in VASP by us. It was already successfully used to study the adsorption geometry and bonding mechanism of pyridine on Cu(110) and Ag(110) surfaces.[48]

III. RESULTS

A. DBQA molecule and monolayer in vacuum

DBQA in the gas phase. The N,N′-di(*n*-butyl)quinacridone molecule is relaxed from the crystal molecular structure[49] (see Fig. 1). The highest lying KS orbitals exhibit very small density on the butyl chains of the molecule which is consistent with the observation of small local density of states (LDOS) values suggested by the experiment[16] (Fig. 2). In the crystal configuration the π cores of the molecules are planar and stacked over one another. In plane they form hydrogen bonds CO···H-C with a bonding distance of 2.52 Å.[49] The molecule is noncentrosymmetric in the crystal, but our DFT calculations reveal that a centrosymmetric version of the molecule in vacuum is more stable by 19 meV when compared to its noncentrosymmetric counterpart in vacuum.

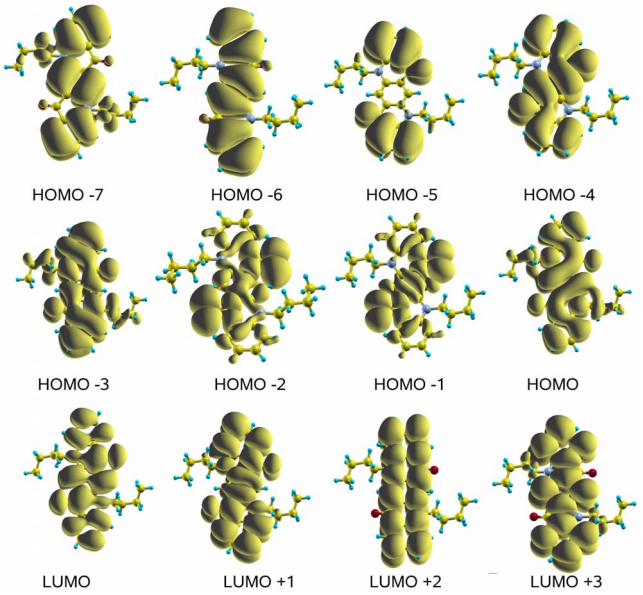

FIG. 2. (Color online) The KS orbitals of the DBQA molecule in the gas phase from HOMO−7 through LUMO+3.

The two butyl chains lie on different sides with respect to the molecular core. As this will certainly alter the adsorption process it was suggested that the chain might rotate away from the surface to enable a planar adsorption of the molecule on the surface. This feature is proposed by molecular mechanics calculations on this system.[50] We therefore also rotated one butyl chain upwards and found that the energy changed insignificantly when comparing the final configurations. The molecular states from HOMO−7 to LUMO+3 also showed no significant difference between the two configurations which is consistent with the low spatial density of states at the butyl chain sites.

Isolated DBQA monolayer. To study the molecule-molecule interaction, we constructed a unit cell containing two DBQA molecules as proposed by experimental results of the surface unit cell.[16] Starting from the relaxed geometry of the molecule from the crystal data we found that the molecular cores oriented in a out-of-plane fashion. The relaxation seems to be dominated by the repulsion of the butyl chains, and we could not find conclusive evidence for hydrogen bonding on the C=O···H-C sites, as there was no charge-density increase along the proposed bond and the C-H bond length did not increase. However it should be noted that due to our larger theoretical Ag bulk lattice constant of 4.165 Å instead of the experimental value of 4.079 Å (Ref. 51) the unit cell was larger by 0.344 Å along [001] and 0.364 Å along $[1\bar{1}0]$ direction. Because of this the molecule-molecule

TABLE I. Binding energies and dipole moments of the two monolayers in vacuum configurations and the four monolayer-substrate configurations studied. For the adsorbed molecular layers the calculated work-function shift $\Delta\phi$ is also given. The labels are used throughout the text. For the different adsorption geometries see Fig. 3.

	Binding energy		Dipole moment (e Å)		Work-function change (eV)	
Configuration	PBE	PBE+D	PBE	PBE+D	PBE	PBE+D
DBQA monolayer, arm down	−0.181	−0.517	0.0	0.0		
DBQA monolayer, arm up	−0.133	−0.498	−0.255	−0.407		
Arm down, oxygen on hollow site (1)	−0.229	−1.903	−0.769	−1.185	−0.48	−0.74
Arm up, oxygen on hollow site (2)	−0.316	−1.904	−0.668	−1.029	−0.42	−0.64
Arm down, oxygen on top site (3)	−0.377	−2.193	−1.362	−1.205	−0.85	−0.75
Arm up, oxygen on top site (4)	−0.492	−2.271	−1.308	−1.157	−0.81	−0.72

distance was increased by 0.17 Å yielding an O···H distance of 3.13 Å and weakening the possible H bonding. The binding energy of the molecules was also small at 181 meV/molecule. The DOS and the spatial distribution of the states were also practically unchanged upon monolayer formation.

To more closely resemble the adsorbed monolayer structure, we also calculated a monolayer of DBQA molecules starting from the relaxed configuration of the DBQA molecule with both arms pointing upwards. In this case the molecular backbones do not tilt out of plane, but we also see no evidence of H bonding. The adsorption energy in this case is 133 meV/molecule. Also the effect on the DOS and the spatial distribution of the frontier orbitals was very small. We thus conclude that at the level of DFT-PBE the intermolecular interaction is weak.

Role of the vdW interactions. The calculations including the dispersion corrections (DFT-PBE+D) showcase their importance for the binding energy for large macromolecules. The intramolecular "energy correction" due to the inclusion of the dispersion correction amounts to 1.4395 eV, a rather large value that exemplifies the difficulties exhibited by dispersion correction schemes such as the one used here[17] concerning atomization energies. The intermolecule binding energy upon monolayer formation increases to 517 meV/molecule. The relaxed geometry for the "arm down" monolayer showed a decrease in the out-of-plane tilting, and for both configurations the butyl chains were closer to the molecular plane.

B. Monolayer on the substrate geometry and adsorption energies

Without vdW interactions. We studied four different starting geometries for the adsorption of the DBQA monolayer onto the substrate, two geometries with the oxygen atoms of the DBQA molecule above the on-top sites of the substrate, and two geometries with the oxygen atoms above the hollow sites. For each of these cases one geometry was with both butyl groups pointing away from the surface ("arm up" configuration) and one geometry starting from the crystal structure of DBQA which means that one of the butyl groups points toward the surface ("arm down" geometry). For the labeling of these structures in the following, see Table I and Fig. 3.

In general, it is observed that the oxygen atoms form a chemical bond with the Ag(110) when they lie above the surface atoms of the substrate (configurations 3 and 4) and they do not bind to it when they are at the hollow site (configurations 1 and 2). This observation is consistent with a similar trend observed for formate[52] and terephthalic acid[53] on the Cu(110) surface or for PTCDA on the Ag(111) one.[11,54] The molecular planes are twisted in the Ag-O bonded cases because the oxygen atoms on opposite sites are nearer to the surface than the rest of the molecular backbone. Note that a similar behavior was observed for PTCDA on Ag(111).[11,54] Another trend observed is that the butyl groups are repelled by the substrate, thereby tilting the molecular backbone out of plane. From an energetic point of view, the binding of the oxygen atoms is the dominating process in terms of total energy, so that the configuration with the oxygen atoms on top of first-layer Ag atoms and the butyl groups pointing away from the substrate is the most stable configuration (configuration 4) while that with one butyl chain toward the substrate is the second most stable (configuration 3). In these two Ag-O bonded cases the π system of the molecule is also much nearer to the surface by about 0.7–0.9 Å (see C1-Sub and C2-Sub distances in Table II). Also, for these two adsorption configurations the backbone is slightly bent in a bridgelike fashion with the center ring further away from the surface than the rings at the end. Additionally, in the cases where one butyl chain points toward the substrate the backbone is further tilted by the repulsion of this butyl chain. Note that the binding energy in the most stable configuration 4 is much higher than the monolayer binding energy, indicating that the molecule-substrate interaction is dominating over the molecule-molecule interaction. This is also evident from the very different relaxation patterns observed.

Role of the vdW interactions. The four configurations discussed above were also relaxed including the dispersion corrections. In general, the addition of the dispersion forces leads to higher binding energies of the monolayer and a

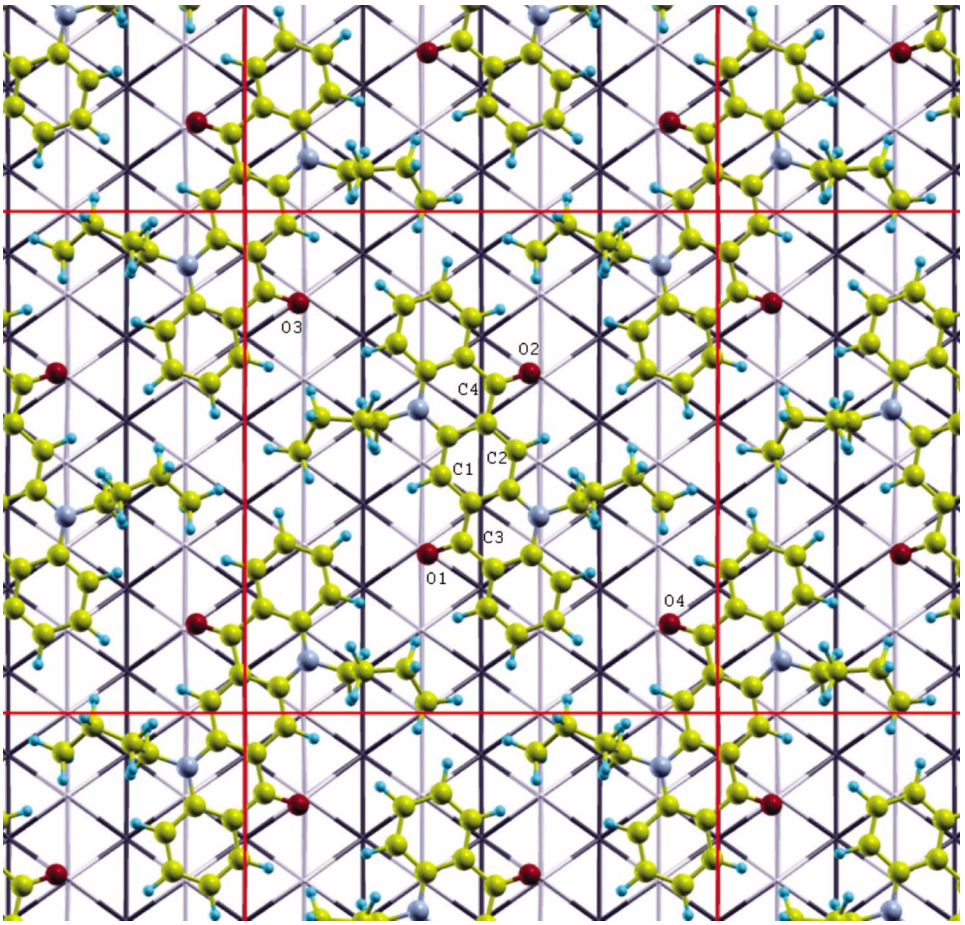

FIG. 3. (Color online) Geometry of the monolayer configurations. The bright substrate atoms are first layer, the dark ones are second layer Ag atoms. Configuration 4 is shown here, configuration 2 is obtained by shifting the substrate to the left by half a lattice constant, so that the oxygen atoms are above the second row atoms. For configurations 1 and 3 one of the butyl chains of each molecule is rotated by 180°. In configurations 1 and 2 all oxygen atoms are in hollow positions of the substrate; in configurations 3 and 4 they are at on top positions.

larger interaction between the molecules and the substrate. It can be seen from Table I that the dispersion corrections led to an increase in the binding energy of about 1.6 eV, a value rather constant about the different adsorption configurations. Nevertheless, its absolute value is larger than the DFT-PBE binding adsorption energy by a factor of 3–8. It can thus be concluded that the dispersion corrections as used in this work—albeit dominating the total energy—are indeed, as often proposed, very site unspecific. In agreement with this energy corrections, also the adsorption geometry shows a clear trend due to a stronger binding to the substrate. The distance between the π-molecular plane as measured by the distance from the two inner C atoms of the molecular core and the substrate decreases on average by 0.7–0.8 Å for configurations 1 and 2 and by 0.25 Å for configurations 3 and 4 (see the C1-Sub and C2-Sub distances in Table II). Also the Ag-O bond length is decreased by about 0.06 Å, and a very slight increase in the C=O double bond length is observed for all adsorption geometries investigated in our study.

C. Monolayer on the substrate-bonding pattern

Without vdW interactions. To study the bonding mechanism of the molecules to the substrate we analyzed the charge-density difference induced on the molecules as well as on the surface n_{diff} upon adsorption. Therefore, the charge density of the molecular monolayer n_{DBQA} in the configuration that is obtained by relaxing it on the substrate and the substrate charge density $n_{\mathrm{Ag(110)}}$ in this configuration are subtracted from the charge density of the whole relaxed system $n_{\mathrm{DBQA+Ag(110)}}$:

TABLE II. The bond lengths for the four configurations studied by conventional DFT with the PBE exchange-correlation energy functional and with additional dispersion corrections. The "bond lengths" labeled C1-Sub and C2-Sub are the distances only along the surface normal of the atoms C1 and C2 to the topmost substrate plane.

	Bond lengths (Å)							
	DFT-PBE				DFT-PBE+D			
Bond	(1)	(2)	(3)	(4)	(1)	(2)	(3)	(4)
Ag-O1	4.18	4.47	2.44	2.48	3.85	3.49	2.39	2.41
Ag-O2	4.11	4.11	2.46	2.44	2.73	3.67	2.41	2.39
Ag-O3	4.35	4.61	2.45	2.48	3.94	3.49	2.39	2.41
Ag-O4	4.33	4.46	2.46	2.44	3.03	4.06	2.41	2.39
C1-Sub	4.04	4.06	3.30	3.10	3.47	3.27	3.05	2.84
C2-Sub	3.98	3.91	3.11	3.10	3.09	3.26	2.90	2.84
C3-O1	1.276	1.277	1.296	1.298	1.277	1.280	1.300	1.304
C4-O2	1.277	1.276	1.299	1.298	1.290	1.277	1.305	1.304

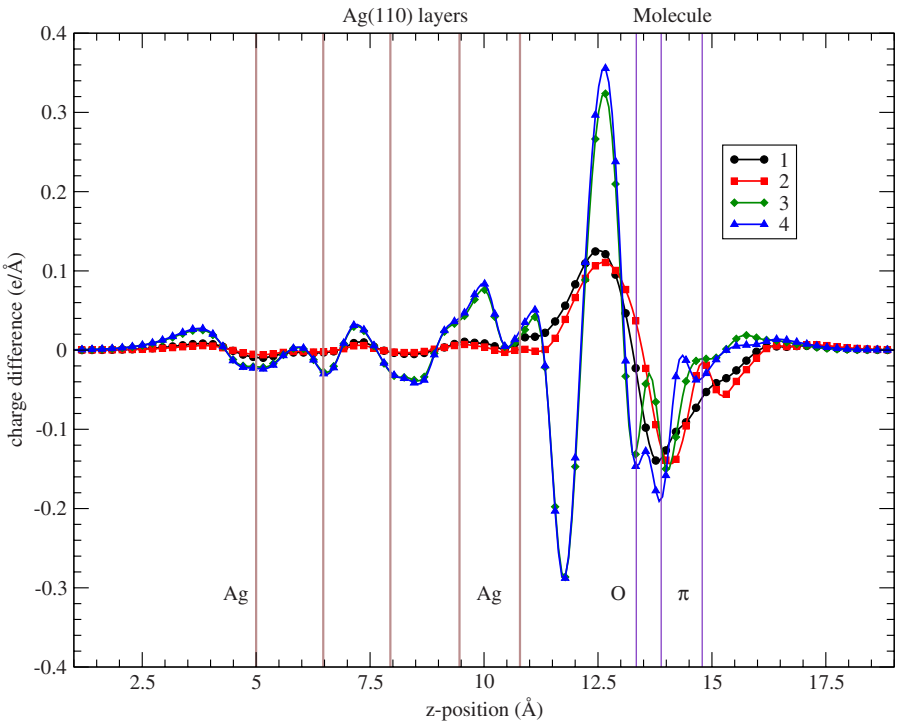

FIG. 4. (Color online) Charge-density difference of all four configurations upon adsorption averaged over planes perpendicular to the surface normal (no dispersion corrections included). The light gray lines mark the positions of the Ag layers of the substrate, the dark (purple) lines mark (from left to right) the positions of the oxygen atoms in configurations 3 and 4, the position of their π core (3.1 Å above the surface) and the position of the π core in configurations 1 and 2 (4.1 Å above the surface).

$$n_{\text{diff}} = n_{\text{DBQA+Ag(110)}} - n_{\text{DBQA}} - n_{\text{Ag(110)}}. \quad (6)$$

Averaging this charge-density difference in a plane perpendicular to the substrate normal yields Fig. 4. It is apparent from Fig. 4 that indeed some charge densities are redistributed in all cases, generating a surface dipole. The general picture of the charge redistribution in configurations 1 and 2 can be rationalized in terms of Pauli repulsion: the molecule-surface interaction effectively pushes the surface electrons closer to the substrate.[55] In configurations 3 and 4 this effect is even more pronounced since the whole molecule is closer to the surface. However, in these cases the charge redistribution pattern is more complicated due to the additional presence of chemical interactions. In particular, in the case of the geometries 3 and 4 one can observe a significant charge depletion near the surface combined with a large charge accumulation near the DBQA molecule (see also below). Looking at isosurfaces of the charge-density difference reveals that the main charge redistribution occurs at the oxygen sites, the Ag atom beneath it, as well as the carbon atoms where the oxygen is bound and the two central carbon atoms of the innermost ring (C1 and C2). Charge accumulation occurs mainly directly beneath the oxygen atoms and the innermost ring; charge depletion mainly above the Ag atom where the oxygen atoms are bonded. A spatial visualization of the charge accumulation pattern is depicted in the isosurface plots of Fig. 5. There are also some charge redistributions away from the C=O double bond inside the DBQA molecule, e.g., a shift of electron density from the bonding region to the atoms. In conclusion, the bonding of the oxygen atom to the substrate involves mainly a charge-density transfer from the substrate and the C=O double bond to the Ag-O bonding region. However, there is also a less pronounced bonding pattern between the central ring and the substrate.

The charge redistribution leads to the formation of a dipole upon bond formation. This surface dipole modifies the work function of the molecule-surface system when comparing to the bare Ag(110) substrate. From a physical point of view, the modification of the surface work function upon atomic or molecular adsorption[10,56,57] is the result of a charge transfer between the adsorbate and substrate together with a charge-density redistribution over the whole molecule-surface interface. The work function $\phi^{\text{DBQA+Ag(110)}}$ of the molecule-substrate interface is given by

$$\phi^{\text{DBQA+Ag(110)}} = V_{\text{vac}}^{\text{up}} - E_F \quad (7)$$

with E_F the Fermi energy and $V_{\text{vac}}^{\text{up}}$ the potential to the left of the potential jump shown in Fig. 6. This potential jump is due to a compensating dipole layer introduced to correct for the dipole-dipole interaction of neighboring slabs. The work-function change due to the adsorption of a monolayer of DBQA molecules $\Delta\phi$ is then calculated as

$$\Delta\phi = \phi^{\text{DBQA+Ag(110)}} - \phi^{\text{Ag(110)}}. \quad (8)$$

The work function calculated for the bare Ag(110) slab is 4.06 eV, below the experimental value of 4.52 eV,[58] but similar to the 4.13 eV obtained by DFT-PBE.[59] As the charge-density difference in Fig. 4 extends to the whole slab we also calculated the work function at the bottom of the Ag slab to judge the influence of the strong molecular interaction in configurations 3 and 4 on the soundness of our slab model. We found that it differs by no more than 0.05 eV from the value of the clean surface and thus the thickness of our slab is large enough to reliably describe the bonding mechanism of DBQA on the Ag(110) surface. In Fig. 6 the plots of the local electrostatic potentials averaged over planes parallel to the surface are shown. To gain an insight into the mechanism of the change of work function of the clean surface due to molecule-substrate interactions, we will return to the analysis of the charge-density difference plots reported in Fig. 4. One

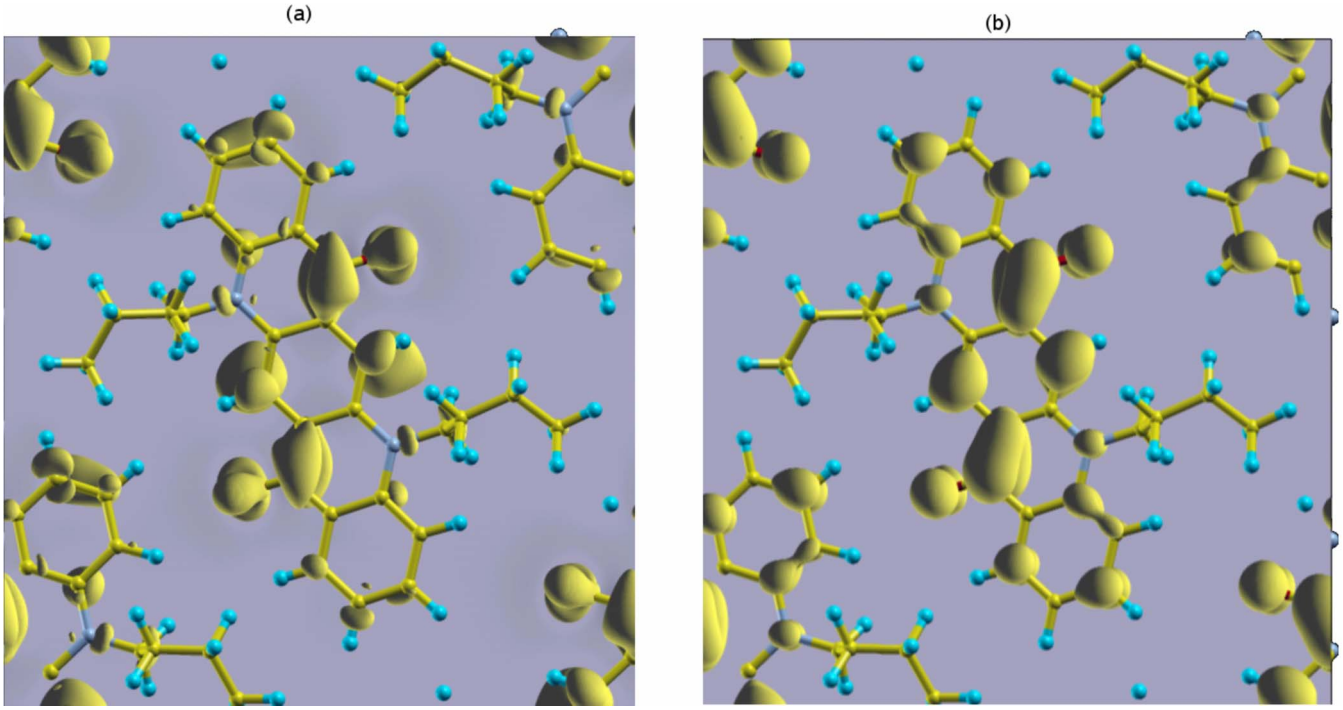

FIG. 5. (Color online) Bonding pattern. (a) The charge-density difference n_{diff} on the molecule in the configuration 4, showing the charge increase under the O atoms and the middle C atoms, compared to (b) the total charge density $n_{\mathrm{DBQA+Ag(110)}}$ obtained by integrating the local density of states in an energy interval that can be identified as the molecular LUMO (see also Fig. 7). One can observe that the charge-density accumulations are mainly located in regions with significant local density of states of the LUMO. For better visibility the charge-density depletion which is mainly located at the C=O double bond and above the Ag atoms where the O atoms are bound is not shown in (a).

can observe two different patterns of charge redistribution of the DBQA-Ag(110) surface system. As already mentioned, the Pauli repulsion effect due to molecule-surface interaction leads to a significant charge redistribution at the molecule-substrate interface which in turn induces a reduction of the intrinsic surface dipole of the clean Ag(110) surface. Besides this, in the case of configurations 1 and 2, the charge transfer from the molecule to the surface (≈0.1 electrons) leads to a decrease of the work function of the clean surface by 0.48 and 0.42 eV, respectively. Note that the amount of charge density transferred from molecule to surface (or vice versa) depends on the definition where the molecule ends and the

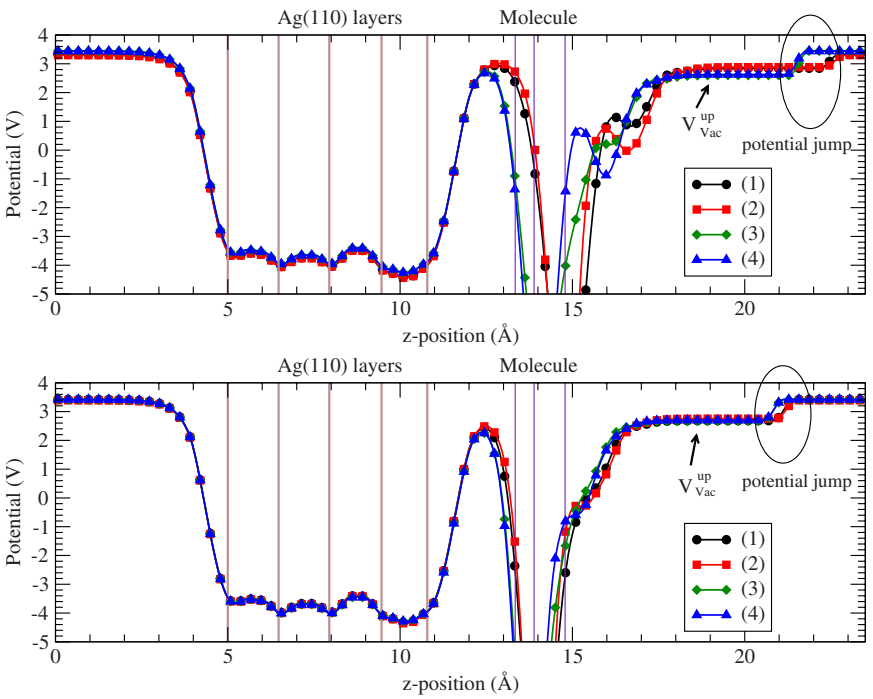

FIG. 6. (Color online) Electrostatic potential averaged over *x-y* planes (perpendicular to surface normal) for each adsorption geometry. The potential jump at the far right of the plots is due to the inclusion of a dipole layer in our *ab initio* calculations to compensate the dipole formed at the molecule-surface interface.

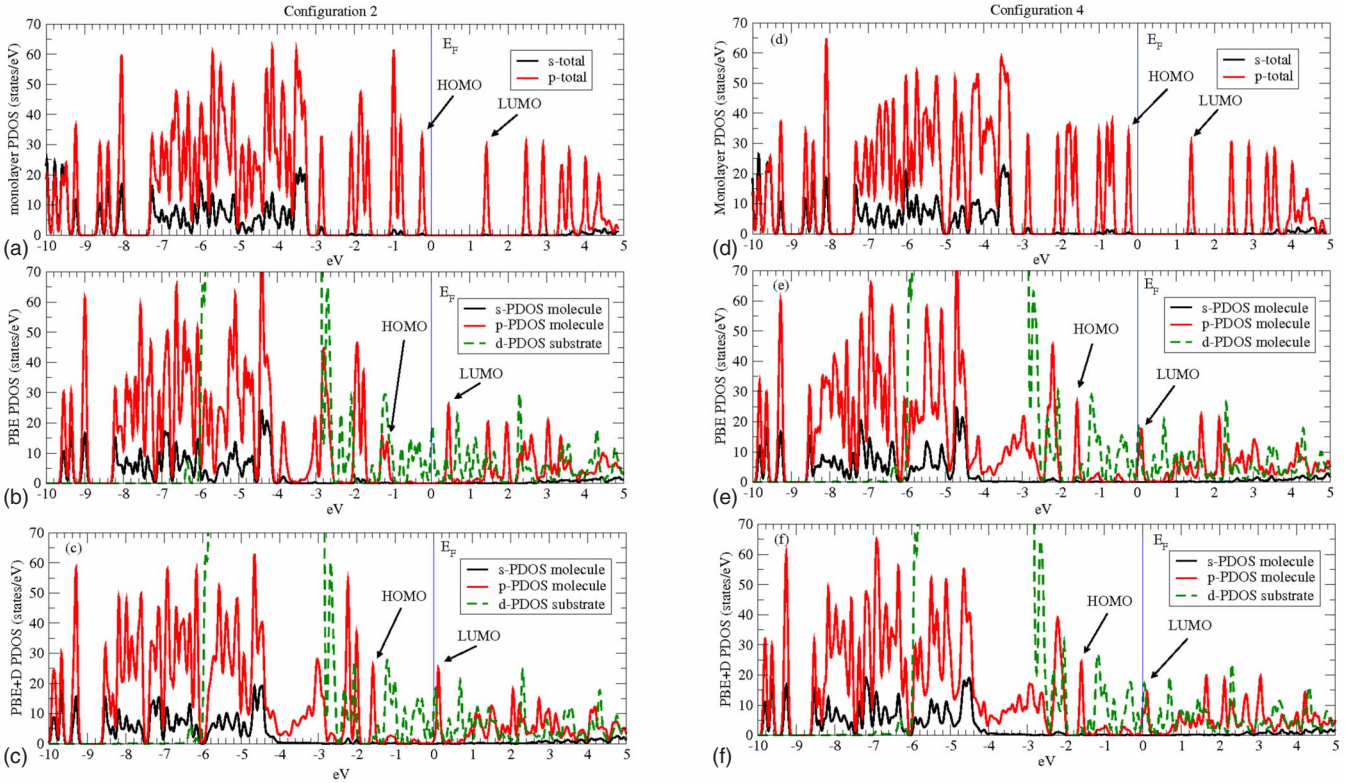

FIG. 7. (Color online) The partial density of states of the monolayer in vacuum and that of the relaxed monolayer-substrate system for configurations 2 (a)–(c) and 4 (d)–(f) with and without dispersion corrections. The first row of graphs [(a) and (d)] represents the PDOS of the monolayer in vacuum, obtained by projecting the total *s*- and *p*-density of states onto all atoms in molecule and summing up. The second and third rows contain the PDOS obtained with PBE and PBE including dispersion corrections, respectively. For comparison, the density of states projected onto the substrate *d* states is also shown. For configuration 2 one can observe a close resemblance of the PDOS depicted in (a) and (b), indicating a small influence of the substrate on the molecular states. In (c), due to the inclusion of the dispersion effects, the LUMO of the molecule is moved toward the Fermi energy, indicating partial occupation of this molecular orbital. Comparing PDOSs shown in (d) and (e), the stronger influence of the substrate in the bonded configuration 4 becomes visible. The lower lying molecular states hybridize strongly with the substrate *d* states, although HOMO and LUMO resemble the molecular states quite closely. The graph (f) shows that the inclusion of the dispersion corrections leads to a small change of the electronic structure of the Ag-O bonded configuration 4.

surface starts and thus such an estimate is rather a qualitative one. Nevertheless, in the case of configurations 3 and 4, a larger amount of charge is accumulated near the molecules ($\approx 0.2\ e$) while a similar amount of charge is depleted near the surface. This charge rearrangement in the region between the monolayer and Ag(110) surface leads to the formation of the series of surface dipoles with the overall effect of a substantial decrease of the bare Ag(110) work function by 0.85 and 0.81 eV, respectively. Besides this, a common feature of all adsorption configurations analyzed in our study reveals a charge depletion as well as a charge accumulation process at the molecular sites, being an additional proof of a complex molecular-surface interaction pattern.

To fully understand the electronic structure of the DBQA-Ag(110) interface, a closer look at the density of states is necessary. The question of interest is how the discrete states of the DBQA molecule evolve upon monolayer formation and adsorption on the Ag(110) surface. As depicted in Figs. 7(a) and 7(d), it is found that the molecular states are only very slightly altered due to the formation of a monolayer in vacuum because of the small molecule-molecule interaction. This conclusion can be drawn by comparing the DOS of the distorted monolayer in vacuum with the DOS of the isolated molecule (not shown). There is a very good one-to-one correspondence between the spatial distribution of the frontier molecular states (in the energy range of $-3-+3$ eV around the Fermi energy) and the states of the monolayer, which are almost always doubly degenerate. Only orbitals which are very close in energy and have a significant density at the oxygen atom sites rehybridize. This is the case, for example, for the HOMO-1, HOMO-2, HOMO-4, and HOMO-5 highest occupied molecular orbitals.

While the electronic KS states of the isolated monolayer can be traced back to their molecular origin quite well, the binding to the substrate renders this process more difficult, as can be seen clearly in Fig. 7. To find the molecular states in these systems, the total DOS of the monolayer adsorbed to the substrate is projected onto the atoms of the molecule (projected density of states, PDOS). The charge density with a specific angular momentum in certain energy intervals is then compared to relevant states of the DBQA monolayer system to figure out how these molecular orbitals develop upon adsorption. As a general feature, the PDOS of the adsorbed molecules resembles that of the isolated monolayer

much more closely in the case of the configurations without Ag-O bonding (geometries 1 and 2). In these unbound cases, the electronic structure of the monolayer is not influenced much by the presence of the substrate, while in the bonded cases (configurations 3 and 4) a significant change in the PDOS is observed, pointing out a stronger molecule-surface interaction in the latter case.

In all adsorption configurations considered in our study but geometry 2 [see Fig. 7(b)], the highest occupied molecular orbital (HOMO) is pretty much unaltered by the presence of a substrate which can be traced back to the absence of significant *d*-state DOS of the substrate in this energy range. Nevertheless, the states below the HOMO are significantly broadened in configurations 3 and 4 due to the presence of the substrate *d* bands [for configuration 4, see Fig. 7(e)]. They form groups, made up of HOMO-7–HOMO-4 in the energy range from −3.7 to −2.5 eV and HOMO-3–HOMO-1 from −2.4 to −2.0 eV. The broadening of the molecular orbitals in this energy range corresponds to a hybridization with the surface *d* states. Note also that for the adsorption geometry 4, the molecular orbitals are shifted to lower binding energies than in the case of configuration 2 [compare Figs. 7(b) and 7(e), respectively] leading to a lower adsorption energy in the first case (see also Table I).

The lowest unoccupied molecular orbital (LUMO) is shifted to the Fermi level and partially occupied during adsorption in case of the configurations 3 and 4 (but not in the case of the adsorption geometries 1 and 2). This observation is in line with the charge back donation of the substrate to the molecule observed in the charge-density plots. As shown in Fig. 5, the spatial charge-density accumulation indeed corresponds well to the LUMO spatial distribution. Thus the bonding pattern of the DBQA monolayer on the Ag(110) surface in the ground state (configuration 4) can be interpreted as a delocalized process of the charge donation from the DBQA to the molecule-surface interface together with a back-donation charge transfer from the surface to the molecular LUMO.

Role of the vdW interactions. The influence of the dispersion corrections on the charge-density difference and the density of states is rather small in case of the Ag-O bonded configurations 3 and 4, but larger for the unbonded geometries 1 and 2. This observation is exemplified by the comparison of the PDOS plots of configurations 4 and 2, with and without dispersion corrections, shown in Fig. 7. Due to the dispersion forces, the DBQA molecules come closer to the substrate in 1 and 2 which leads to a shift of the LUMO toward the Fermi energy and its partial occupation. Therefore, a smaller molecule-surface distance yields a charge transfer from the substrate to the molecule. The decreasing molecule-surface distance also induces a stronger Pauli-repulsion effect. In configuration 1 a localized chemical bond between one of the oxygen atoms (O2) and the substrate is formed although this atom is above the hollow position of the substrate. In the case of the adsorption geometry 2 there is no localized bond, but still the LUMO is shifted to the Fermi energy and becomes partially occupied due to the approach of the molecule to the substrate as a result of the dispersion forces. Also the work-function change $\Delta\phi$ for configurations 1 and 2 increases for these adsorption geometries (see Table I) due to a larger Pauli repulsion effect in combination with a larger charge transfer between the monolayer and the surface, yielding a larger surface dipole when dispersion corrections are included. This effect emphasizes the importance of the dispersion forces to calculate the work-function modifications of physisorbed systems. In 1 the increase is more pronounced than in 2, which can be attributed to the existence of an additional Ag-O bond in the first case. Interestingly, the molecular core is also brought closer to the surface in configurations 3 and 4 by the dispersion forces but this process is accompanied by a decrease of the surface dipole and the work-function change, as no significant additional charge transfer occurs.

IV. SUMMARY

By using density functional theory including semiempirical dispersion corrections, we have investigated the adsorption of a monolayer of N,N′-di(*n*-butyl)quinacridone on Ag(110) in an adsorption geometry suggested by an experimental study[16] of this system. By studying four different adsorption geometries it was shown that the site recognition of the oxygen atoms to first-layer Ag atoms is the dominating process governing the adsorption geometry and the conformation of the butyl chain was of relatively smaller importance. The most stable geometry, however, is indeed the one predicted earlier by molecular dynamics with the butyl chains pointing away from the surface.[50]

Although the bonding pattern can be understood mainly as a localized process of Ag-O bond formation, one can also explain this process as a charge donation of the substrate to the more delocalized molecular LUMO. This process is possible because the adsorption of DBQA on the Ag(110) surface shifts this state to the Fermi energy where it becomes partially occupied. Also, the charge-density difference plot reveals charge-density increases that correspond well to the spatial extent of the LUMO. This bonding pattern was previously found in the similar systems of PTCDA on Ag(111),[54] NTCDA on Ag(110),[59] and THQ on Ag(111).[12]

The dispersion corrections led to a rather large increase in the atomization energy of the DBQA molecule in vacuum. Increases in the binding energy of the molecules to the substrate were dramatic, yet site unspecific. Thus the energy ranking of the four configurations remained the same as for DFT-PBE calculations, i.e., the adsorption geometry 4 is the ground-state one. Even in the Ag-O bound cases the semiempirical dispersion energy is much larger than the DFT-PBE part of the binding energy. The distance between the molecules and the substrate was also decreased by as much as 0.7–0.8 Å for the "unbound" configurations and 0.25 Å for the bound ones. The influence of this correction on chemical bond lengths was negligible though, as it should be. Also the effect on the DOS and the charge-density distribution was small for the bonded cases. However, for configurations without chemical bonds to the substrate the approach of the molecule to the substrate leads to a stronger push-back effect on the surface electrons as well as a partial occupation of the molecular LUMO which is shifted to the Fermi energy. Hence a significant charge redistribution is induced

which has an important influence on the surface dipole and thus on the work-function change. For the bonded configurations the work function of the clean Ag(110) surface decreased due to the lack of significant additional charge donation and the decreasing distance of the molecular core to the substrate.

We can thus conclude that dispersion corrections of the form used here have a possibly large influence on the geometry, especially in regions of very flat potential-energy surfaces, and the binding energy. The effect on the electronic structure of chemically bound species is rather small, but larger on unbound ones. We observed no change in the energy ranking of the different configurations, which we can attribute to the fact that all studied adsorption geometries were equally flat. Nevertheless, because of the magnitude of these corrections, they can be expected to strongly favor flat adsorption geometries over upright ones.

ACKNOWLEDGMENTS

The computations were performed with the help of the ZIVCLUSTER (University of Münster) and the Superdome of the Physical Institute of University of Münster. This work was financially supported by DFG within the framework of the international collaborative Projects No. TRR61 and No. SFB 424.

*chi@uni-muenster.de

[1] *Organic Light-Emitting Devices*, edited by J. Shinar (Springer-Verlag, New York, 2004).
[2] M. A. Reed, C. Zhou, C. J. Muller, T. P. Burgin, and J. M. Tour, Science **278**, 252 (1997).
[3] C. Joachim, J. K. Gimzewski, and A. Aviram, Nature (London) **408**, 541 (2000).
[4] M. Elbing, R. Ochs, M. Koentopp, M. Fischer, C. von Hänisch, F. Weigend, F. Evers, H. B. Weber, and M. Mayor, Proc. Natl. Acad. Sci. U.S.A. **102**, 8815 (2005).
[5] M.-K. Ng, D.-C. Lee, and L. Yu, J. Am. Chem. Soc. **124**, 11862 (2002).
[6] C. D. Dimitrakopoulos, S. Purushothaman, J. Kymissis, A. Callegari, and J. M. Shaw, Science **283**, 822 (1999).
[7] C. Dimitrakopoulos and P. Malenfant, Adv. Mater. (Weinheim, Ger.) **14**, 99 (2002).
[8] V. C. Sundar, J. Zaumseil, V. Podzorov, E. Menard, R. L. Willett, T. Someya, M. E. Gershenson, and J. A. Rogers, Science **303**, 1644 (2004).
[9] G. Heimel, L. Romaner, J.-L. Brédas, and E. Zojer, Phys. Rev. Lett. **96**, 196806 (2006).
[10] G. Heimel, L. Romaner, E. Zojer, and J.-L. Brédas, Nano Lett. **7**, 932 (2007).
[11] M. Rohlfing, R. Temirov, and F. S. Tautz, Phys. Rev. B **76**, 115421 (2007).
[12] M. Abel, V. Oison, M. Koudia, and L. Porte, Phys. Rev. B **77**, 085410 (2008).
[13] L. W. Bruch, R. D. Diehl, and J. A. Venables, Rev. Mod. Phys. **79**, 1381 (2007).
[14] D. C. Langreth, M. Dion, H. Rydberg, E. Schröder, P. Hyldgaard, and B. I. Lundqvist, Int. J. Quantum Chem. **101**, 599 (2005).
[15] M. Dion, H. Rydberg, E. Schröder, D. C. Langreth, and B. I. Lundqvist, Phys. Rev. Lett. **92**, 246401 (2004).
[16] F. Lin, D. Y. Zhong, L. F. Chi, K. Ye, Y. Wang, and H. Fuchs, Phys. Rev. B **73**, 235420 (2006).
[17] S. Grimme, J. Comput. Chem. **27**, 1787 (2006).
[18] G. Kresse and J. Hafner, Phys. Rev. B **47**, 558 (1993).
[19] G. Kresse and J. Furthmüller, Comput. Mater. Sci. **6**, 15 (1996).
[20] G. Kresse and J. Furthmüller, Phys. Rev. B **54**, 11169 (1996).
[21] J. P. Perdew, K. Burke, and M. Ernzerhof, Phys. Rev. Lett. **77**, 3865 (1996).
[22] J. Ireta, J. Neugebauer, and M. Scheffler, J. Phys. Chem. A **108**, 5692 (2004).
[23] P. E. Blöchl, Phys. Rev. B **50**, 17953 (1994).
[24] G. Kresse and D. Joubert, Phys. Rev. B **59**, 1758 (1999).
[25] W. Kohn, Y. Meir, and D. E. Makarov, Phys. Rev. Lett. **80**, 4153 (1998).
[26] Y. Andersson, D. C. Langreth, and B. I. Lundqvist, Phys. Rev. Lett. **76**, 102 (1996).
[27] E. Hult, Y. Andersson, B. I. Lundqvist, and D. C. Langreth, Phys. Rev. Lett. **77**, 2029 (1996).
[28] B. Lundqvist, Y. Andersson, H. Shao, S. Chan, and D. Langreth, Int. J. Quantum Chem. **56**, 247 (1995).
[29] K. Rapcewicz and N. W. Ashcroft, Phys. Rev. B **44**, 4032 (1991).
[30] H. Iikura, T. Tsuneda, T. Yanai, and K. Hirao, J. Chem. Phys. **115**, 3540 (2001).
[31] M. Kamiya, T. Tsuneda, and K. Hirao, J. Chem. Phys. **117**, 6010 (2002).
[32] T. Sato, T. Tsuneda, and K. Hirao, J. Chem. Phys. **123**, 104307 (2005).
[33] T. Sato, T. Tsuneda, and K. Hirao, Mol. Phys. **103**, 1151 (2005).
[34] J. F. Dobson and B. P. Dinte, Phys. Rev. Lett. **76**, 1780 (1996).
[35] M. Lein, J. Dobson, and E. Gross, J. Comput. Chem. **20**, 12 (1999).
[36] M. A. Basanta, Y. J. Dappe, J. Ortega, and F. Flores, Europhys. Lett. **70**, 355 (2005).
[37] M. Elstner, P. Hobza, T. Frauenheim, S. Suhai, and E. Kaxiras, J. Chem. Phys. **114**, 5149 (2001).
[38] L. Zhechkov, T. Heine, S. Patchkovskii, G. Seifert, and H. A. Duarte, J. Chem. Theory Comput. **1**, 841 (2005).
[39] X. Wu, M. C. Vargas, S. Nayak, V. Lotrich, and G. Scoles, J. Chem. Phys. **115**, 8748 (2001).
[40] Q. Wu and W. Yang, J. Chem. Phys. **116**, 515 (2002).
[41] U. Zimmerli, M. Parrinello, and P. Koumoutsakos, J. Chem. Phys. **120**, 2693 (2004).
[42] A. D. Becke and E. R. Johnson, J. Chem. Phys. **122**, 154104 (2005).
[43] A. D. Becke and E. R. Johnson, J. Chem. Phys. **123**, 154101 (2005).
[44] M. A. Neumann and M.-A. Perrin, J. Phys. Chem. B **109**, 15531 (2005).
[45] F. Ortmann, F. Bechstedt, and W. G. Schmidt, Phys. Rev. B **73**, 205101 (2006).

[46] S. Grimme, J. Antony, T. Schwabe, and C. Mück-Lichtenfeld, Org. Biomol. Chem. **5**, 741 (2007).
[47] S. Grimme, J. Comput. Chem. **25**, 1463 (2004).
[48] N. Atodiresei, V. Caciuc, J.-H. Franke, and S. Blügel, Phys. Rev. B **78**, 045411 (2008).
[49] K. Ye *et al.*, J. Phys. Chem. B **109**, 8008 (2005).
[50] D. X. Shi *et al.*, Phys. Rev. Lett. **96**, 226101 (2006).
[51] W. P. Davey, Phys. Rev. **25**, 753 (1925).
[52] N. Atodiresei, K. Schroeder, and S. Blügel, Phys. Rev. B **75**, 115407 (2007).
[53] N. Atodiresei, V. Caciuc, K. Schroeder, and S. Blügel, Phys. Rev. B **76**, 115433 (2007).
[54] A. Hauschild, K. Karki, B. C. C. Cowie, M. Rohlfing, F. S. Tautz, and M. Sokolowski, Phys. Rev. Lett. **94**, 036106 (2005).
[55] P. S. Bagus, V. Staemmler, and C. Wöll, Phys. Rev. Lett. **89**, 096104 (2002).
[56] H. Ishii, K. Sugiyama, E. Ito, and K. Seki, Adv. Mater. (Weinheim, Ger.) **11**, 605 (1999).
[57] A. Michaelides, P. Hu, M.-H. Lee, A. Alavi, and D. A. King, Phys. Rev. Lett. **90**, 246103 (2003).
[58] H. B. Michaelson, J. Appl. Phys. **48**, 4729 (1977).
[59] A. Alkauskas, A. Baratoff, and C. Bruder, Phys. Rev. B **73**, 165408 (2006).